This article has been accepted for publication in a future issue of this journal, but has not been fully edited. Content may change prior to final publication. Citation information: DOI 10.1109/ACCESS.2017.2765181, IEEE Access

PAM and CAP-based Transmission Schemes for Visible-Light Communications

Mohammad Ali Khalighi [1], Shihe Long [1], Salah Bourennane [1], Zabih Ghassemlooy [2]

[1] Aix Marseille University, CNRS, Centrale Marseille, Institut Fresnel, Marseille, France

[2] Optical Communications Research Group, NCR Lab, Faculty of Engineering & Environment, Northumbria University, Newcastle upon Tyne, UK

Email: *Ali.Khalighi@fresnel.fr*

***Abstract*—Visible light communications (VLC) have received extensive attention in the research community thanks to their advantages of high bandwidth, low cost, robustness to electromagnetic interference, operation in an unregulated spectrum, and high degree of spatial confinement in indoor scenarios. One of the main limitations for high data-rate transmission in VLC systems is the limited modulation bandwidth of commercial light emitting diodes. To circumvent this limitation, spectrally-efficient modulation schemes should be used. Optical orthogonal frequency-division multiplexing (O-OFDM) based schemes have become very popular and several proofs of concept have shown their ability to attain over-Gbps transmission rates. We consider here the use of pulse amplitude modulation and carrier-less amplitude and phase modulation schemes together with frequency-domain equalization (FDE) at the receiver as interesting alternatives to O-OFDM. We show the advantages of the former schemes in terms of the peak-to-average power ratio, and demonstrate through numerical results the merits of FDE-based signaling in attaining high data rates.**

***Index Terms*—Visible-light communications; Optical OFDM; pulse amplitude modulation; carrierless amplitude and phase modulation; frequency-domain equalization, PAPR.**

I. Introduction

In the past decade, world has witnessed a dramatic increase in the data traffic and demand for high-speed Internet services such as HDTV, video calls, and cloud computing. This has strengthened the need for further innovation, research and development in new emerging wireless technologies capable of delivering high transmission rates. The development of novel and efficient wireless technologies for different transmission scenarios and link distances is essential for building future heterogeneous communication networks to support a wide range of service types and to meet the ever-increasing demand for higher data rates. This in particular concerns the 5th generation telecommunication networks where ubiquity and ultra-high spectral efficiency are among the main features [1].

Given the exponential growth in the wireless data rates, existing communication standards will be unable to satisfy the increasing demand for data throughput. In particular, in an Internet-of-things or Internet-of-everything paradigm, the current radio frequency (RF) transmission standards may not address all challenges and requirements. By harnessing the optical spectrum, optical wireless communications (OWC) have been shown to be a powerful complementary technology to the new RF transmission standards [2].

A. Visible Light Communications

An interesting application area of OWC is in indoor environments where an important part of the wireless traffic takes place. In particular, the visible light communications (VLC) technology aims at using the incoherent solid-state lighting devices such as light emitting diodes (LEDs) for illumination, data transmission (with a promise of over-Gbps data rates), and indoor localization. By exploiting the LED-based illumination facilities for data transmission, the VLC technology provides a unique opportunity to provide communications in underground and mining environments, to provide high security (in banking and finance, manufacturing, and military), and to avoid electromagnetic radiations in restrictive areas (such as hospitals and within aircrafts) and at the same time permits a significant reduction in power consumption of the users [3], [4]. This application of VLC has been recently called Li-Fi (light fidelity) that can be seen as an example of the "green communication," which effectively exploits high energy-efficient LED lighting ($> 70\%$ compared to standard lighting sources) for data transmission, we can avoid/limit power-hungry alternative solutions such as Wi-Fi networks, particularly in indoor environment; thus, reducing the pressure on the RF spectrum so that it could be used in areas where mobility is paramount. Note that, some recent works have considered the use of VLC for indoor localization and sensing as well. According to [5], the global market for VLC is expected to grow at a compound annual growth rate of 109.2% from 2015 to 2022.

B. Indoor VLC

LEDs are expected to be the primary illumination source in the future thanks to the advances made in incoherent solid-state lighting and because of significantly reduced energy consumption compared to the traditional lighting sources, and the possibility of easy control of intensity and color of illuminated spaces. In VLC, LED luminaries are exploited for simultaneous illumination, broadband data transmission and indoor localization. The most relevant case is white light illumination where a popular approach consists in using the so-called white LEDs, where a blue LED is used together with yellowish phosphor coating to emit a broad-spectrum white light. These devices have the main advantage of reduced

This article has been accepted for publication in a future issue of this journal, but has not been fully edited. Content may change prior to final publication. Citation information: DOI 10.1109/ACCESS.2017.2765181, IEEE Access

production cost but at the price of reduced bandwidth (i.e., $3-5$ MHz compared to 20 MHz of red, green and blue LEDs) [6], [7]. Several proofs-of-concept have been realized recently showing the possibility of high transmission rates [7]–[9]. A next generation OWC standard is currently defined (i.e., IEEE 802.15.7r1), which aims at data rates within the range of 1 Mbps - 10 Gbps. Hwever, despite the numerous advantages of this technology, the commercial deployment of VLC is far from being straightforward.

In this paper, we focus on the downlink and discuss appropriate transmission solutions that can allow high data rate transmission. We start by a brief overview of techniques for high data rate transmission for VLC links in Section II. Among these techniques, we focus on optical orthogonal frequency-division multiplexing (O-OFDM) -based transmissions in Section III and discuss their pros and cons. Next, in Section IV we consider single-carrier transmission solutions as an alternative to O-OFDM. For these schemes, we propose to use frequency domain equalization, as described in Section V. The performance of the proposed schemes is investigated in Section VI through a set of numerical results. Lastly, concluding remarks and some discussions are given in Section VII.

II. High-rate data transmission by VLC

The most important limiting factor in increasing the data rate of VLC systems is the relatively low modulation bandwidth of commercial GaN-based white LEDs (typically $<$ 5 MHz), which is due to the slow response time of the coated phosphorous. One solution to increase the bandwidth is to use a blue filter at the receiver (Rx) to remove this slow component from the modulated signal. By doing so, the modulation bandwidth can be increased up to 20 MHz typically [2], [10], but at the cost of an increased intensity loss on the order of 10 dB, which could be tolerable in practice as we have in general a sufficiently high signal-to-noise ratio (SNR) at the Rx (i.e., > 70 dB) due to the illumination level recommended by the European Lighting Standard [7]. Other proposed solutions are pre- or post-equalization [11], using multiple-input multiple-output (MIMO) structures [12]–[15], and high-order modulation schemes based on O-OFDM [10], [16]–[18]. In particular, the MIMO technology through employing spatial multiplexing can effectively boost the data-rate. Note that, in contrast to RF or free-space optics counterparts where MIMO is used to increase link reliability by providing spatial diversity gain against channel fading [19], [20], in indoor VLC systems we are mostly concerned with a deterministic channel [21], [22], and hence, the only interest of adopting MIMO architectures is to increase the data rate through spatial multiplexing. The simple way of implementing a MIMO link is to use a non-imaging lens at the Rx for collecting the transmitted intensity. But the drawback is that the channel matrix may become rank-deficient or ill-conditioned depending on the Rx position, in which cases, data recovery at the Rx becomes rather impossible [12]. The use of an imaging lens can circumvent this problem at the price of increased size, cost and complexity of the Rx [2].

As such, the use of O-OFDM for achieving higher data rate R_d in VLC systems has drawn particular attention and it has even become omnipresent in most related publications. The highest reported R_d (laboratory set-ups) are around 1 Gbps for the case of white LEDs and about 3 Gbps for the case of RGB LEDs over a range of several tens of centimeters typically [7], [9]. Recently, some researches have considered the use of GaN-based micron-size LEDs (commonly called μLEDs) that have the advantage of very large modulation bandwidths (typically a 3-dB bandwidth of 60 MHz), and have demonstrated peak data rates around 3.5 Gbps [8].

III. O-OFDM-based data transmission

OFDM is a well-known spectrally efficient technique for achieving high data-rate transmission over frequency-selective RF channels. This multicarrier transmission technique offers a simple way to divide the entire channel into a number of narrow-band sub-channels and to multiplex data over them, thereby allowing an increase in the symbol duration and a reduction of the inter-symbol interference (ISI). In fact, due to the need for very high R_d, most of today's RF systems are suffering from multipath induced ISI, and hence, OFDM has become a popular technique to simplify the channel equalization task at the Rx.

This idea has inspired the researchers working in VLC to deal with the limited bandwidth of the LEDs. This scheme is known as O-OFDM, or optical discrete multi-tone (DMT). At the same time, O-OFDM is a robust solution against channel frequency selectivity that mostly occurs either when a line-of-sight (LOS) path is not available due to blockage or shadowing, thus resulting in a *diffuse* channel inducing a relatively large delay spread, or when multiple LOS paths exist (from multiple emitters to the Rx) [21]. Basically, through the insertion of a cycle prefix (CP) at the beginning of each frame of OFDM symbols, the frequency-selective *aggregate* channel (including the effects of the propagation channel and the LED response) is equalized using a simple single-tap equalizer. To increase further the R_d, bit and power loading can be introduced in order to match the data rate of different sub-channels to the frequency response of the aggregate channel [17], [18], [23].

A. Most popular O-OFDM schemes

Given that intensity modulation with direct detection (IM/DD) is widely used in VLC systems due to the highly non-coherent LED sources, the information-bearing signal has to be real and positive prior to IM of the LED. Several transmission schemes based on O-OFDM have been proposed so far, the most popular being DC-biased O-OFDM (DCO-OFDM) and asymmetrically-clipped O-OFDM (ACO-OFDM) [16], [24]. In both schemes, Hermitian symmetry is imposed on the modulated subcarriers to guarantee a real time-domain OFDM signal. In the former scheme, a DC bias is added to the signal to make it unipolar. Obviously, this cannot be guaranteed to hundred percent unless a very large DC bias is used, which results in a poor energy efficiency. Thus, with a DC bias, the remaining negative amplitudes are clipped (i.e., set to zero) prior to IM, which is usually modeled by the so-called clipping noise (CN) [25]. In ACO-OFDM, on the other

This article has been accepted for publication in a future issue of this journal, but has not been fully edited. Content may change prior to final publication. Citation information: DOI 10.1109/ACCESS.2017.2765181, IEEE Access

hand, only the odd sub-carriers are modulated and the even subcarriers are assigned zero amplitude. In this way, the time domain signal will have an anti-symmetric property, which is then made positive by hard clipping the negative part. By doing so, the resulting CN affects only the even sub-carriers and not the data carrying (odd) sub-carriers [16], [26].

To achieve the same R_d, DCO-OFDM needs a much smaller constellation size than ACO-OFDM, e.g., m-QAM (quadrature amplitude modulation) for the former, and m^2-QAM for the latter. Let us denote the symbol rate and the normalized LED bandwidth by R_S and B_{LED}, respectively. This way, for relatively small values of $\eta = R_S/B_{\text{LED}}$, ACO-OFDM offers an improved optical power efficiency than DCO-OFDM, whereas for larger η, DCO-OFDM is more power efficient.

B. Drawbacks of O-OFDM

In O-OFDM schemes there are a number of drawbacks, which have motivated researchers to investigate alternative more robust transmission solutions. Basically, the optimality of the O-OFDM schemes is rather questionable, in particular, regarding spectral efficiency. Firstly, the Hermitian symmetry constraint incurs a spectral-efficiency loss of factor two and four for DCO-OFDM and ACO-OFDM, respectively, compared with baseband unipolar modulation schemes such as pulse amplitude modulation (PAM) [27]. CP insertion also reduces slightly the spectral efficiency. Another major drawback is the relatively high peak-to-average power ratio (PAPR) of the O-OFDM-based schemes. In fact, given the limited linear operation range of most commercial LEDs, the corresponding double-side signal clipping, to fit the signal into the LED dynamic range (DR), can severely affect the system performance. This is especially the case for high modulation orders where the system can suffer from severe non-linear distortion, i.e., high CN.

A few variants of O-OFDM have recently been proposed such as the enhanced unipolar OFDM (eU-OFDM) [28] that promises similar spectral efficiency as DCO-OFDM with almost no DC power penalty. Also, pilot-assisted transmission was proposed in [29] in order to reduce the PAPR. These schemes generally imply a considerable increase in the system complexity, as compared to DCO-OFDM, for instance.

IV. Alternative solutions to O-OFDM

Some other modulation schemes have recently been under investigation such as PAM and carrier-less amplitude and phase (CAP) modulation. The well-known PAM, which uses a certain number of discrete amplitudes for transmitting data, is a "baseband" transmission scheme where the spectral centroid of the signal that modulates the LED intensity is located at the zero frequency. The "bandpass" CAP modulation, on the other hand, is basically a QAM modulation where instead of using a mixer for up- and down-conversion, employs two orthogonal finite impulse response (FIR) digital filters whose impulse responses (IRs) form a Hilbert-transform pair [27]. This way, the electrical signal that modulates the LED intensity is a DC-biased QAM signal on a sub-carrier of relatively low frequency. Historically, CAP was considered for high data rate signal transmission over telephone cables for asymmetric digital subscriber line (ADSL) connections [30] before being withdrawn in favor of DMT. It was considered for optical communication in [26] and more recently revisited in the contexts of optical fiber transmission [31]–[34] and VLC [35]–[38] thanks to its advantages of low PAPR and a simple system structure.

Figure 1 illustrates the principle of CAP. For the case of analog CAP signaling, Fig. 1(a), the real (I: In-phase) and imaginary (Q: Quadrature) parts of QAM-modulated symbols are passed through two orthogonal filters $h_I(t)$ and $h_Q(t)$, which are related through the Hilbert transform [39] to realize the frequency shifting. We have:

$$h_I(t) = g(t)\,\cos(2\pi f_c t), \quad h_Q(t) = g(t)\,\sin(2\pi f_c t), \quad (1)$$

where $g(t)$ is the IR of the baseband shaping filter, which is usually a square-root raised-cosine (SRRC) function. To ensure the orthogonality of I and Q filters, f_c should be larger than the maximum frequency of $g(t)$. The signal at the output of the modulator can be written as:

$$s(t) = \sum_{n=-\infty}^{\infty} i[n]\,h_I(t-nT) - q[n]\,h_Q(t-nT) \quad (2)$$

where $i[n]$ and $q[n]$ are the corresponding I and Q symbols after QAM mapping.

In the digital implementation (see Fig. 1(b)), this is done using the equivalent FIR digital filters $h_I[n]$ and $h_Q[n]$. In order to increase the precision of this digital pulse shaping, inputs to these filters are first up-sampled by a factor M by inserting $(M-1)$ zeros between consecutive symbols. The precision of these filter depends also on the number of filter taps L_f used in their implementation. By setting M and L_f to sufficiently large values, we can obtain performance close to the ideal analog case, i.e. when using $h_I(t)$ and $h_Q(t)$. Otherwise, this pulse shaping would not satisfy the Nyquist criterion (inducing hence undesired ISI) and in addition, will result in non-zero cross-correlation between $h_I[n]$ and $h_Q[n]$ inducing, hence, cross-talk between I and Q branches.

We have shown in Fig. 2(a) the IRs of $h_I[n]$ and $h_Q[n]$ filters as well as their auto- and cross-correlation for $M = 8$. We can neglect the tails of these IRs by taking a sufficiently large L_f. For instance, setting $L_f = 20$ and $M = 8$, we effectively use 161 filter taps, which has an obvious impact on the system computational complexity.

In the following, we will consider the same SRRC filtering for the case of PAM signaling in order to make a fair comparison between its performance and that of CAP. Note that in contrary to the baseband PAM, CAP is a passband signal, as it can be seen from Fig. 3 that shows the spectra of the two signals for a given symbol duration T_S.

Indeed, the most important advantage of PAM and CAP over O-OFDM is their lower PAPR (thus, being less subjected to CN). At the same time, they have the advantages of higher spectral efficiency and lower power consumption at the transmitter (Tx). However, at higher data rates they may suffer from significant ISI where the aggregate channel becomes frequency-selective. This means that channel

This article has been accepted for publication in a future issue of this journal, but has not been fully edited. Content may change prior to final publication. Citation information: DOI 10.1109/ACCESS.2017.2765181, IEEE Access

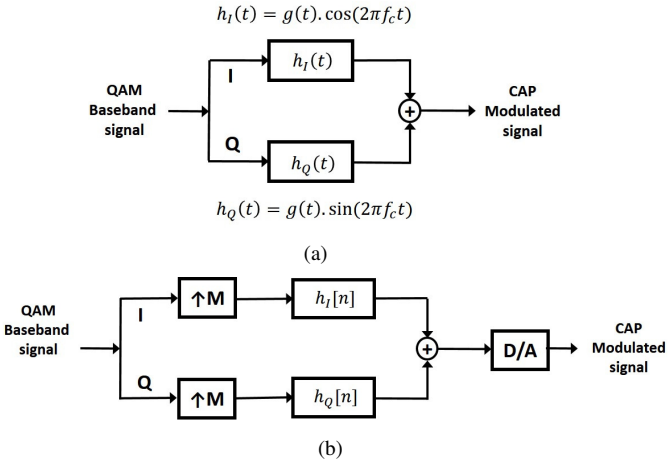

Fig. 1: Principle of CAP signaling: (a) basic CAP transmitter using analog filters where $h_I(t)$ and $h_Q(t)$ have the role of up-converting the baseband signal; (b) CAP transmitter using digital filters, a large enough up-sampling factor M increases filters' accuracy.

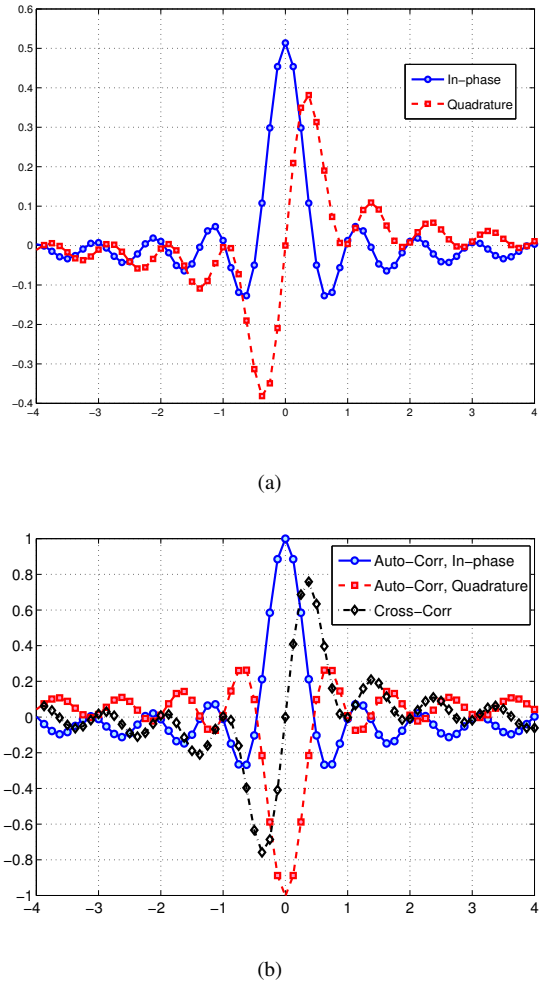

Fig. 2: CAP signaling, (a) in-phase and quadrature filters' IRs for $M = 8$; (b) autocorrelations and cross-correlation of I and Q IRs. Pulse shaping $g(t)$ is a square-root raised cosine SRRC filtering with 0.1 roll-off factor. The abscissa is normalized by the symbol duration T_s.

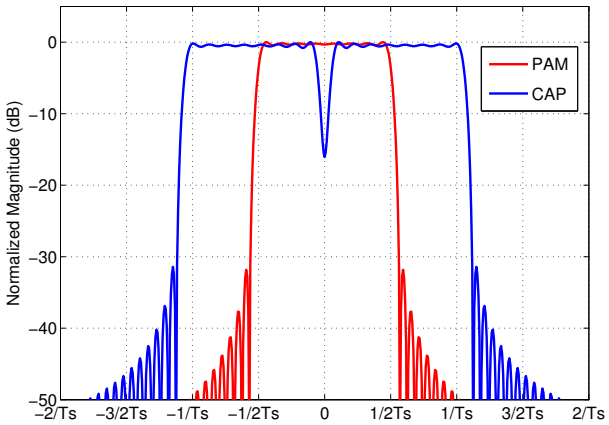

Fig. 3: Spectrum of CAP signal compared to PAM, T_s denotes symbol duration.

equalization has to be performed at the Rx prior to signal de-mapping. Channel equalization is classically performed in the time domain, which is in general complex to implement. We consider here frequency-domain equalization (FDE) under block transmission, which has the advantage of relatively low computational complexity and necessitates a single-tap equalizer together with fast-Fourier transform (FFT) / inverse FFT (IFFT) operations over the frame at the Rx [40]–[42].

V. FDE-BASED TRANSMISSION USING PAM AND CAP

Before describing PAM and CAP transmission schemes, let us briefly present the rather classical case of DCO-OFDM transmission; see Fig. 4(a). At the Tx, the information bits are modulated using a QAM constellation. The Hermitian symmetry is then applied to the time-domain symbol frame before applying an IFFT and inserting a CP of length L. To limit the signal bandwidth, SRRC pulse-shaping is then applied to the signal. Next, double-side clipping is applied prior to digital-to-analog (D/A) conversion, adding a DC bias, and IM of the LED. Denoting the modulated signal by $x(t)$, the DC bias current is set as $k\sqrt{\mathrm{E}\{x(t)\}^2}$, where $\mathrm{E}\{.\}$ denotes expectation and k is the clipping level, which is related to the so-called clipping factor κ, defined as: $\kappa = 10\log_{10}(k^2+1)$. At the Rx, following photo-detection and analog-to-digital (A/D) conversion, digital matched filtering is performed prior to CP removal and FFT. Single-tap channel equalization is then performed and the transmitted bits are recovered after demodulation.

The block diagrams of the Tx and the Rx for PAM and CAP transmission are shown in Figs. 4(b) and 4(c), respectively. For the case of PAM, at the Tx, the mapped symbols are organized into frames of length N and with a CP of length L inserted at the start of each frame to avoid inter-frame interference. Then, after pulse shaping and signal clipping, a DC bias is added to it after D/A conversion to ensure a certain illumination level. For the case of CAP, following QAM mapping and CP insertion to the frames of complex symbols, I and Q components of the symbols are passed through the digital filters $h_I[n]$ and

This article has been accepted for publication in a future issue of this journal, but has not been fully edited. Content may change prior to final publication. Citation information: DOI 10.1109/ACCESS.2017.2765181, IEEE Access

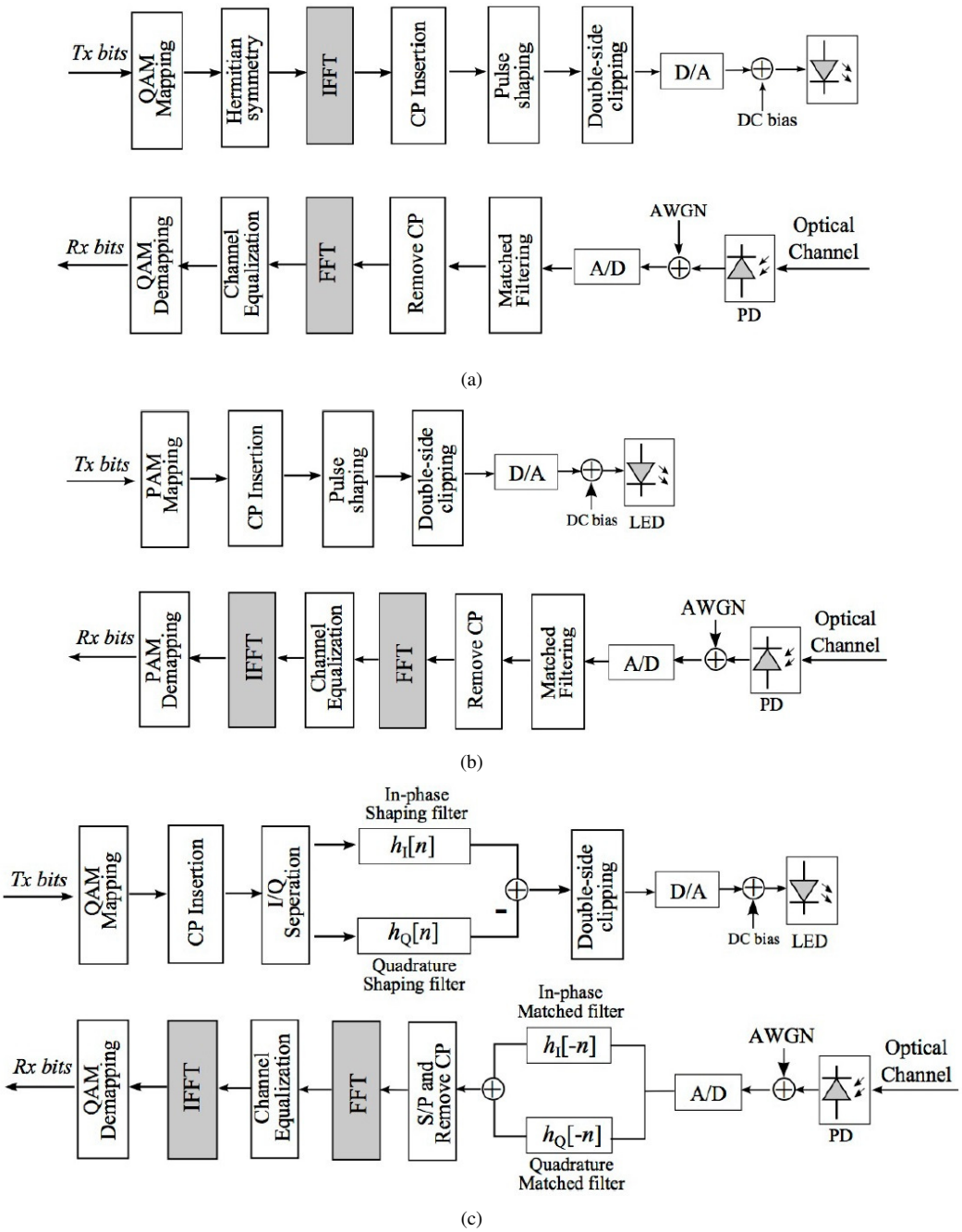

Fig. 4: Block diagrams of the Tx and the Rx: (a) DCO-OFDM, (b) PAM-FDE, and (c) CAP-FDE.

$h_Q[n]$. The output of the subtracter is then passed through double-sided clipping and D/A conversion modules prior to insertion of the DC bias. At the Rx, for both cases, following optical-to-electrical conversion, the received signal is sampled and applied to the digital matched filter. Next, for each frame, after CP removal, channel equalization is carried out in the frequency domain before symbol demapping.

Let us focus in more detail on the pulse shaping and matched filtering operations, which are performed in the digital domain. As explained earlier (see Fig. 1(b)), an up-sampling of factor M is performed before digital filtering by inserting $(M-1)$ zeros between consecutive symbols. The filter output is then down-sampled to reduce computational complexity. For the case of CAP, in order to guarantee a sufficiently low cross-talk between I and Q branches, one would expect that larger L_f and M are required, compared to PAM. Overall, we notice that PAM-FDE and CAP-FDE schemes have the advantage of reduced Tx complexity but need a more complex hardware at the Rx, as compared with DCO-OFDM. However, this is not really an issue, given the availability of advanced digital circuits.

To explore the signal PAPR, let us contrast the corresponding complementary cumulative distribution function (CCDF) plots of the three schemes for different frame sizes. Results are shown in Fig. 5, which testify the advantage of PAM and CAP over DCO-OFDM. For instance, the probabilities that

This article has been accepted for publication in a future issue of this journal, but has not been fully edited. Content may change prior to final publication. Citation information: DOI 10.1109/ACCESS.2017.2765181, IEEE Access

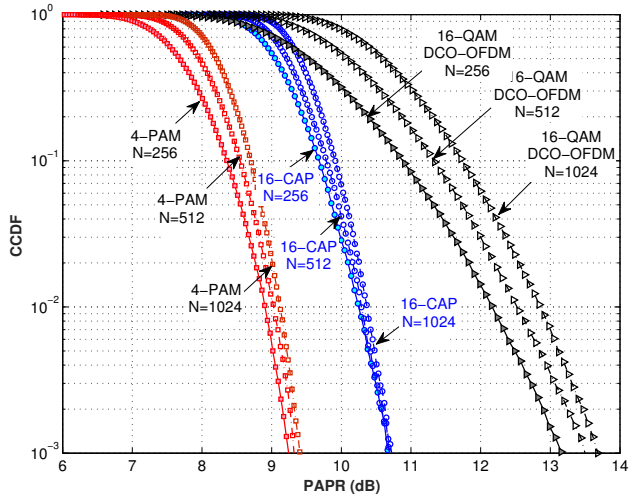

Fig. 5: Contrasting CCDFs of PAPR for PAM- and CAP-FDE and DCO-OFDM for different frame sizes N.

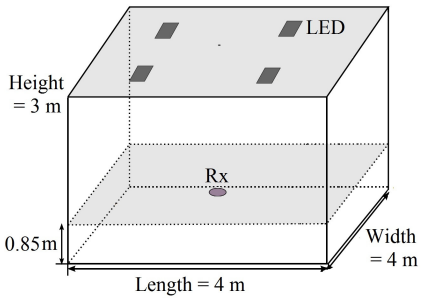

Fig. 6: Illustration of the link configuration considered in the simulations.

TABLE I: Default parameters of the Tx, Rx, and the optical channel.

Parameter	value
Room size ($L \times W \times H$)	$4 \times 4 \times 3$ m^3
Receiver height	0.85 m
LED lamp configuration	2×2, symmetrically arranged
Channel path loss	5×10^{-5}
LED Lambertian order	1
DR of LED drive current I	$0.1 - 1$ A
LED 3-dB modulation bandwidth	2.5 MHz (20 MHz: blue filtering)
Receiver type	PIN
Photo-detector responsivity	1
Receiver noise unilateral PSD N_0	10^{-21} W/Hz
Frame size N	256 symbols
CP length L	8 symbols
Up-sampling factor M	8
Pulse shaping	SRRC of roll-off factor 0.1
Pulse-shaping filter span L_f	20 symbols

the PAPR exceeds 10 dB are about 0.03, and 0.3 for 16-CAP and 16-QAM DCO-OFDM, respectively, whereas it is almost zero for 4-PAM. In addition, the PAPR of DCO-OFDM is very sensitive to the FFT size and increases considerably with N (which corresponds to the number of modulated sub-carriers), whereas for the two other schemes this increase is rather small. Therefore, for increased frame size, the FDE-based schemes do not suffer from any significant increase in PAPR.

VI. Performance Study

In order to get more insight into the perfromance of the FDE-based schemes, we present here a set of Monte-Carlo simulation based numerical results.

A. Indoor channel model and assumptions

We consider a medium-size room of dimension $(4 \times 4 \times 3)$ m^3 with four LED lights positioned symmetrically on the ceiling with respect to the room center, see Fig. 6. The Rx is positioned at the center of the room at a height 0.85 cm above the room floor, which is classically that of a desktop, and uses an optical Rx composed of a PIN photo-detector and a trans-impedance amplifier. We assume that there are no other objects or people within the room to cause beam blocking or shadowing. We consider using OSTAR LEDs from OSRAM with the semi-angle at half power about 65° and model them as Lambertian sources. The channel loss coefficient is 5×10^{-5}. The LED DR corresponds to the current range interval of $0.1\text{A} < I < 1\text{A}$. For the sake of simplicity, we do not consider any clipping factor here and set the DC bias to the DR center, i.e., at I_{DC} of 0.55A. While we take the CN into account, we assume that the LED has a linear characteristic within its DR. Without loss of generality, we normalize the "input current - output optical power" efficiency of the LED. The LED is modeled as a first order low-pass filter with a 3 dB modulation bandwidth of $f_b = 2.5$ MHz with normalized IR of $h_{\text{LED}}(t) = e^{-2\pi f_b t}$. For the sake of comparison, we also consider the case where a blue filter is used at the Rx resulting in an effective modulation bandwidth of 20 MHz [2]. Note that using such a filter also results in a reduction of the background noise level at the Rx. Therefore, without loss of generality, we do not consider any additional power loss due to blue filtering; our aim being to compare the performance of the different schemes under the same channel conditions. Other simulation parameters are summarized in Table I.

Given the transmitted signal $s(t)$, the received signal can be written as follows:

$$r(t) = \gamma\, s(t) \otimes h_{\text{LED}}(t) \otimes h_{\text{VLC}}(t) + \mathsf{n}(t), \qquad (3)$$

where γ is the PD responsivity in (A/W) that is set to unity for simplicity, $h_{\text{VLC}}(t)$ is the IR of the physical indoor VLC channel, and $\otimes$ denotes convolution. Also, $\mathsf{n}(t)$ is the Rx noise, which is modeled as signal-independent additive white Gaussian noise (AWGN) with one-sided power spectral density (PSD) of N_0. We assume that the Rx is background noise limited. We do not use any channel coding and no lens is used at the Rx. Given the link configuration, see Fig. 6, we model $h_{\text{VLC}}(t)$ by a shifted Dirac function (see [21]). Lastly, the SNR being relatively high, we use the classical zero-forcing equalization for which, we obviously need to know the channel IR that we can estimate based on the transmission of pilot symbols. Here, we consider the case where the aggregate channel IR is perfectly known at the Rx.

B. Comparison of PAM- and CAP-FDE with DCO-OFDM

Lets see how these signaling schemes perform in terms of energy efficiency for a given data rate R_d. We have presented

This article has been accepted for publication in a future issue of this journal, but has not been fully edited. Content may change prior to final publication. Citation information: DOI 10.1109/ACCESS.2017.2765181, IEEE Access

in Fig. 7 the bit error rate (BER) plots as a function of electrical power at the Tx, P_{Tx} (excluding the DC power), for $\eta = R_S/B_{\text{LED}} = 5$ and 10. Sub-figures 7(a) and 7(b) correspond to the cases of without and with blue filtering at the Rx. We consider 64-CAP and 8-PAM modulations as well as DCO-OFDM with 64-QAM that provide the same R_d of about 71.5 and 143 Mbps for $\eta = 5$ and 10, respectively. When using blue filtering, R_d will be 570 Mbps and 1.14 Gbps, corresponding to $\eta = 5$ and 10, respectively. Note that we do not consider any bit/power loading for the DCO-OFDM case.

As seen, for a given transmission scheme, the BER decreases by increasing the transmit power P_{Tx} until a limit over which the BER degrades due to the dominance of CN, i.e., signal clipping outside the LED DR (for about $P_{\text{Tx}} \gtrsim -16$ dB). In practice, however, the system will operate within the LED DR and therefore will not use such high P_{Tx} levels. From Fig. 7(a), at a BER of 10^{-3} (i.e., the forward error correction limit) and $\eta = 5$, the power requirements are around -38.7, -32.7, and -31.7 dB for 64-QAM DCO-OFDM, 8-PAM, and 64-CAP, respectively. For $\eta = 10$, CAP outperforms PAM at this BER: the corresponding P_{Tx} values are around -29.7 and -28.3 dB for 64-CAP and 8-PAM, respectively. Note that PAM has the lowest PAPR and suffers from the least CN. Nevertheless, being a baseband modulation, to achieve the same R_d, it needs half of the bit/symbol than CAP, which is a bandpass modulation scheme. As η increases, the channel becomes more and more frequency-selective and the baseband PAM suffers from more attenuation in the relatively high frequency region, compared to the bandpass CAP signal. Under such conditions, CAP provides an improved performance over PAM. We notice similar results when using blue filtering, see Fig. 7(b).

The interesting point is that in both cases, DCO-OFDM outperforms both FDE-based schemes. Indeed, here we intentionally considered a relatively small FFT size $N = 256$ and signal constellation 64-QAM to have the AWGN as the dominant factor affecting the performance. For larger FFT sizes and/or for higher modulation orders, the higher PAPR of DCO-OFDM becomes increasingly penalizing as the CN becomes more and more important. This is illustrated in Fig. 8 where plots of BER versus P_{Tx} are contrasted for different N and different QAM modulation orders. We can see that the performance of the DCO-OFDM scheme can degrade severely for large values of these parameters. Note that the performances of PAM- and CAP-FDE are independent of the frame size N and also have negligible dependence on the constellation size.

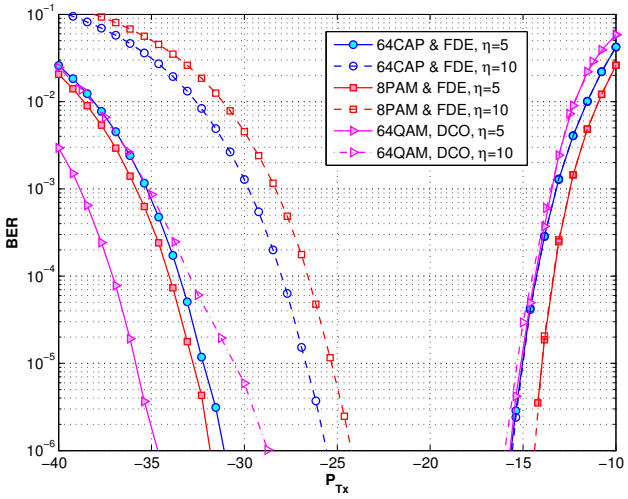

(a)

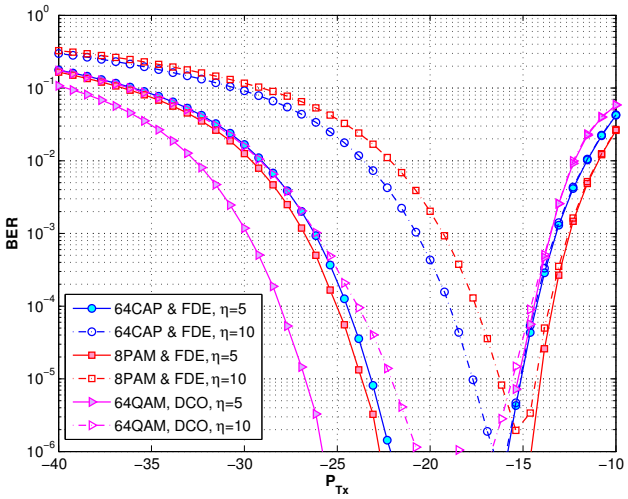

(b)

Fig. 7: Contrasting BER performances of CAP-FDE, PAM-FDE, and DCO-OFDM schemes for: (a) without and (b) with blue filtering at the Rx (B_{LED} of 2.5 and 20 MHz, respectively).

C. FDE-based schemes: Effect of pulse shaping parameters

Let us investigate the influence of the choice of the parameters related to Tx and Rx digital filters, i.e., the up-sampling factor M and the filter span L_f. We have shown in Fig. 9 the BER plots versus P_{Tx} for $\eta = 5$, 10 and three values of M for CAP- and PAM-FDE schemes where no blue filtering is used at the Rx (similar conclusions are drawn when using blue filtering). We notice that the choice of M has a non-negligible impact on the link performance. Almost same results are obtained for For $M \geq 8$. If we tolerate a moderate loss in SNR, we can set a smaller up-sampling factor to reduce the computational complexity. Interestingly, the same sensitivity to M is observed for the case of PAM. Therefore, the main factor affecting the BER is the ISI resulting from imperfect Nyquist filtering rather than non-zero cross-talk between I and Q branches for the case of CAP.

As concerns the choice of filter span, we have contrasted the BER plots in Fig. 10 for CAP- and PAM-FDE schemes and different L_f. Obviously, with a larger L_f, we are closer to the ideal pulse shaping and matched filtering. In this case study, the best performance is obtained for $L_f = 20$ and larger values do not allow any noticeable improvement in the BER. Interestingly, the CAP-FDE scheme appears to be more sensitive to the choice of L_f than PAM. This can be explained by a higher crosstalk between I and Q channels due to non-ideal filtering for the former case.

This article has been accepted for publication in a future issue of this journal, but has not been fully edited. Content may change prior to final publication. Citation information: DOI 10.1109/ACCESS.2017.2765181, IEEE Access

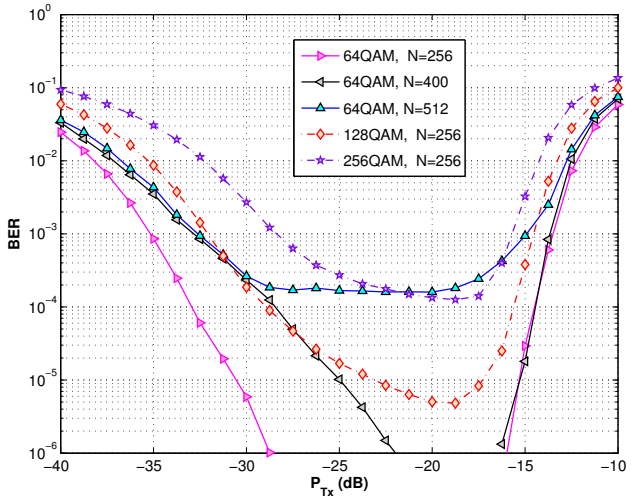

Fig. 8: Performance degradation of DCO-OFDM for increased PAPR: larger FFT size N or larger constellation size. $B_{\text{LED}} = 2.5\,\text{MHz}$, $\eta = 10$.

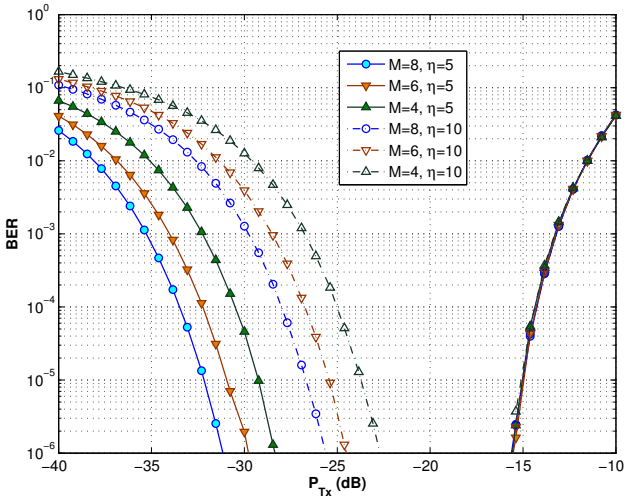

(a)

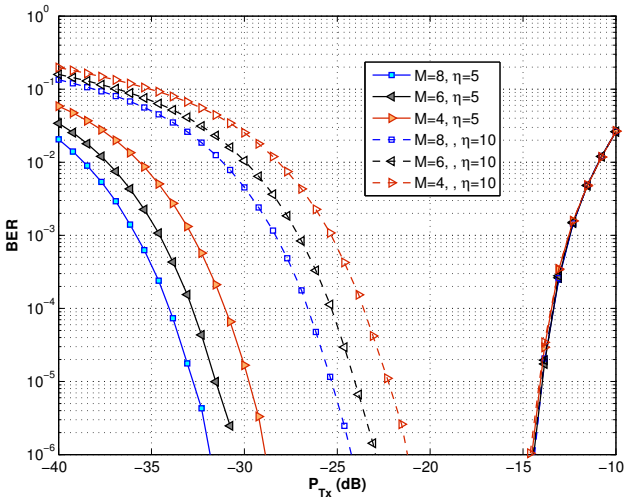

(b)

Fig. 9: Sensitivity of FDE-based transmission schemes to the up-sampling factor M. (a) 64-CAP; (b) 8-PAM. $B_{\text{LED}} = 2.5\,\text{MHz}$. Other parameters correspond to default values in Table I.

D. FDE-based schemes: Effect of CP length

Lastly, let us investigate the importance of the choice of the CP length L on the link performance. Since we have considered a rather simple link configuration where the VLC channel is frequency non-selective, see Fig. 6, only h_{LED} introduces ISI in our case (of course, apart from the ISI induced due to non-ideal pulse shaping and matched filtering). For increased η, we exploit more and more bandwidth of the LED and consequently, the aggregate channel becomes more and more frequency selective. In other words, for increased η, we should use a larger CP.

We have shown in Fig. 11 BER plots for different η and when using different CP values. Let us consider first the case of CAP-FDE, see Fig. 11(a). For $\eta = 5$, a CP of $L = 1$ is sufficient to remove the ISI induced by the channel (larger L result in the same BER performance). For increased η we need to increase L, but given the simple channel we have considered here, the value of CP remains very small; i.e. the corresponding loss in the spectral efficiency is negligible. The required CP lengths for $\eta = 10$ and 20 are $L = 2$ and 6, respectively. For the case of PAM, Fig. 11(b), we notice that we need a larger L, compared to CAP. This can be explained by the fact that PAM is a low-pass signal and for the same η, it spectrum is more affected by the aggregate channel frequency response than CAP, see Fig. 3. The required L for $\eta = 5$ and 10 are 4 and 6, respectively.

VII. Conclusions and Discussions

We investigated FDE-based schemes as alternatives to O-OFDM in the context of indoor VLC systems and elucidated their advantage in dealing with a limited DR of the emitter device. We showed that PAM and CAP have the advantage of lower PAPR, and hence, lower sensitivity to the clipping noise. The latter scheme appears to be more advantageous for higher data rate transmission, i.e., relatively larger ratios of bit-rate to the system bandwidth. As such, FDE-based schemes can be an interesting alternative to O-OFDM, which has usually claimed to be the "evident" solution.

We considered in this paper an ideal (linear) LED characteristic within its DR. In practice, in addition to clipping, the signal undergoes further distortion due to the non-linear "output power - driving current" characteristics of the LED as well as the non-linearity of the power amplifiers (drivers) at the Tx [43]. Given that this nonlinearity affects the system performance especially at high PAPRs, FDE-based schemes are expected to be still more advantageous over O-OFDM.

Concerning the implementation complexity, the IFFT operation at the Tx in O-OFDM-based schemes could be considered as being shifted to the Rx side in FDE-based schemes. This can be considered as the main price paid for benefiting from a lower PAPR. Considering Li-Fi applications, this means less complex lighting installations while necessitating more

This article has been accepted for publication in a future issue of this journal, but has not been fully edited. Content may change prior to final publication. Citation information: DOI 10.1109/ACCESS.2017.2765181, IEEE Access

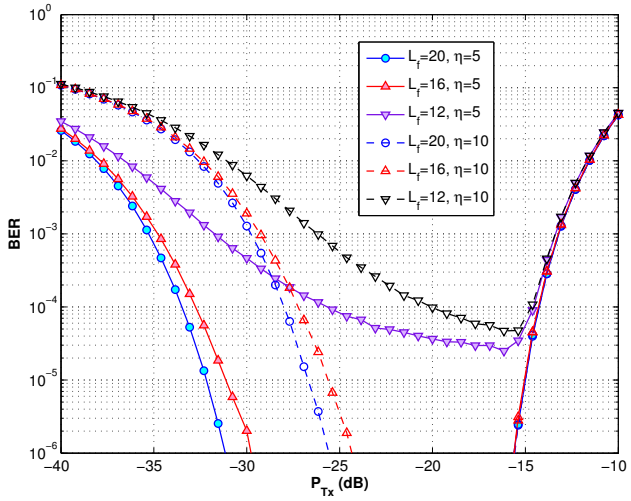

(a)

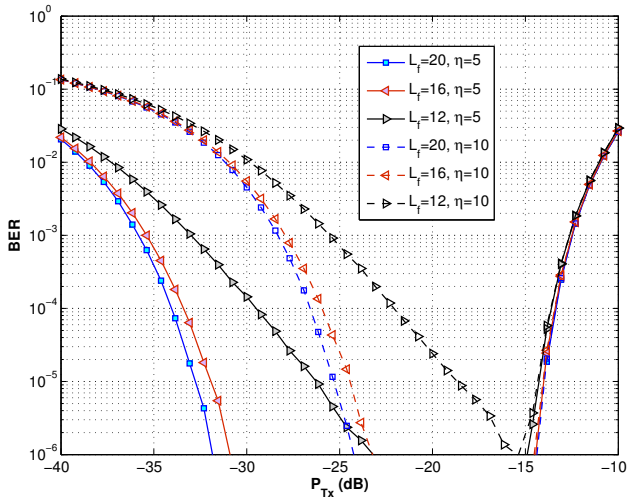

(b)

Fig. 10: Sensitivity of FDE-based transmission schemes to the pulse-shaping filters' span L. (a) 64-CAP; (b) 8-PAM. $B_{\text{LED}} = 2.5\,\text{MHz}$. Other parameters correspond to default values in Table I.

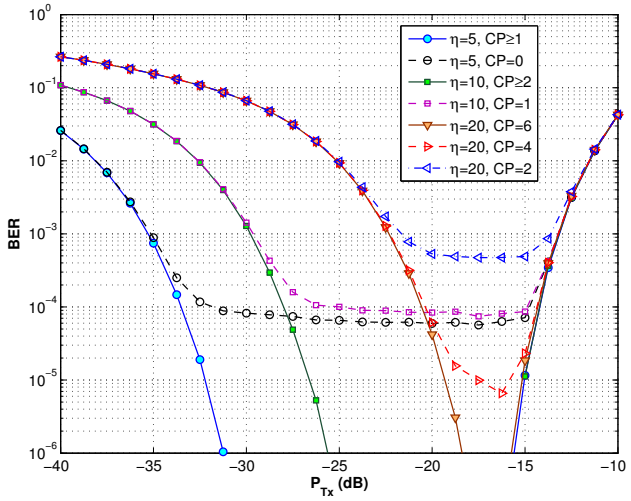

(a)

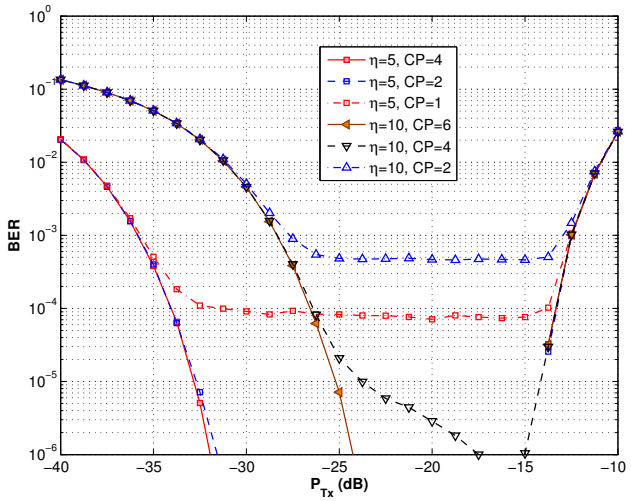

(b)

Fig. 11: Sensitivity of FDE-based transmission schemes to the CP length. (a) 64-CAP; (b) 8-PAM. $B_{\text{LED}} = 2.5\,\text{MHz}$. Other parameters correspond to default values in Table I.

complex Rx devices. The former is an obvious advantage for the deployment of the technology, whereas the latter can be a disadvantage that may be tolerated thanks to the advances in digital integrated circuits and the battery lifetime of the portable devices.

It is worth discussing the choice of SRRC pulse shaping for PAM in our study. By choosing the same pulse shaping for the considered signaling schemes, we wanted to compare their performances with the same optical power at the Tx and the same electrical noise variance at the Rx. In practice, for the case of PAM, a rectangular pulse shape would be preferable since this removes the need for FIR filtering at the Tx. Obviously, the signal will be of much larger bandwidth, but this is not an important issue (in contrary to RF transmission with much more strict bandwidth regulations). Furthermore, one can realize the PAM signaling levels by simply switching on and off different LEDs. On the other hand, the return-to-zero (RZ) signaling format can be used instead of non-RZ (NRZ), which provides a slightly improved performance but at the cost of increased bandwidth requirement [42]. Moreover, one can also combine PAM with line coding to shift the signal spectrum and avoid the DC component. This will ensure a constant short time average of the signal, and hence, a constant LED brightness (that is important or illumination).

Note that, despite the advantage of reduced PAPR for FDE-based schemes, O-OFDM could provide a higher data rate thanks to the possibility of bit and power loading, but at the cost of considerable increased system complexity. In fact, the principle of bit and power loading can also be applied to the case of multi-band CAP signaling (usually called m-CAP) [44]. However, such a scheme requires multiple pulse shaping (and matched filtering) filters to be implemented in

digital domain, which makes the resulting system of rather high implementation complexity. For this reason, the FDE-based schemes proposed here could be of special interest in device-to-device communications.

Although in the presented results we considered not so high data rates, competitive data-rates with Wi-Fi (about two orders of magnitude higher) can be achieved through employing spatial multiplexing using MIMO structures, wavelength division multiplexing (WDM), and using faster emitters such as μLEDs [45]. Meanwhile, it is worth mentioning that, although recent Wi-Fi standards such as IEEE 802.11.ac and .ad promise over-Gpbs data rates, they will likely be exposed to the spectrum congestion problem in the very near future since they use the unlicensed ISM band and with increase in number of Wi-Fi routers, their performance will be limited by packet collisions thus resulting in long back-offs [46].

ACKNOWLEDGMENT

The authors would like to thank Dr. Mike Wolf from Communications Research Laboratory, Ilmenau University of Technology, Ilmenau, Germany, for the fruitful discussions on PAM-FDE transmission.

REFERENCES

[1] M. Ayyash, H. Elgala, A. Khreishah, V. Jungnickel, T. Little, S. Shao, M. Rahaim, D. Schulz, J. Hilt, and R. Freund, "Coexistence of WiFi and LiFi toward 5G: Concepts, opportunities, and challenges," *IEEE Communications Magazine*, vol. 54, no. 2, pp. 64–71, Feb. 2016.

[2] Z. Ghassemlooy, W. Popoola, and S. Rajbhandari, *Optical Wireless Communications: System and Channel Modelling with* MATLAB. CRC Press, 2013.

[3] S. Dimitrov and H. Haas, *Principles of LED Light Communications: Towards Networked Li-Fi*. Cambriage University Press, 2015.

[4] Z. Ghassemlooy, L. N. Alves, S. Zvànovec, and M. A. Khalighi, *Visible Light Communications, Theory and Applications*. CRC Press, 2017.

[5] "Visible light communication market - global industry analysis, size, share, growth, trends and forecast 2015 - 2022," *Transparency Market Research*, Aug. 2014.

[6] A. Jovicic, J. Li, and T. Richardson, "Visible light communication: Opportunities, challenges and the path to market," *IEEE Communications Magazine*, vol. 51, no. 12, pp. 26–32, Dec. 2013.

[7] L. Grobe, A. Paraskevopoulos, J. Hilt, D. Schulz, F. Lassak, F. Hartlieb, C. Kottke, V. Jungnickel, and K.-D. Langer, "High-speed visible light communication systems," *IEEE Communications Magazine*, vol. 51, no. 12, pp. 60–66, Dec. 2013.

[8] D. Tsonev, H. Chun, S. Rajbhandari, J. McKendry, S. Videv, E. Gu, M. Haji, S. Watson, A. Kelly, G. Faulkner, M. Dawson, H. Haas, and D. O'Brien, "A 3-Gb/s single-LED OFDM-based wireless VLC link using a Gallium Nitride μLED," *IEEE Photonics Technology Letters*, vol. 26, no. 7, pp. 637–640, Apr. 2014.

[9] Z. Sun, D. Teng, L. Liu, X. Huang, X. Zhang, K. Sun, Y. Wang, N. Chi, and G. Wang, "A power-type single GaN-based blue LED with improved linearity for 3 Gb/s free-space VLC without pre-equalization," *IEEE Photonics Journal*, vol. 8, no. 3, p. 7904308, Jun. 2016.

[10] J. Grubor, S. Randel, K.-D. Langer, and J. Walewski, "Broadband information broadcasting using LED-based interior lighting," *IEEE/OSA Journal of Lightwave Technology*, vol. 26, no. 24, pp. 3883–3892, Dec. 2008.

[11] P. A. Haigh, Z. Ghassemlooy, H. Le Minh, S. Rajbhandari, F. Arca, S. F. Tedde, O. Hayden, and I. Papakonstantinou, "Exploiting equalization techniques for improving data rates in organic optoelectronic devices for visible light communications," *IEEE/OSA Journal of Lightwave Technology*, vol. 30, no. 19, pp. 3081–3088, Oct. 2012.

[12] L. Zeng, D. C. O'Brien, H. Le Minh, G. E. Faulkner, K. Lee, D. Jung, Y. J. Oh, and E. T. Won, "High data rate multiple input multiple output (MIMO) optical wireless communications using white LED lighting," *IEEE Journal on Selected Areas in Communications*, vol. 27, no. 9, pp. 1654–1662, Dec. 2009.

[13] A. H. Azhar, T.-A. Tran, and D. O'Brien, "A Gigabit/s indoor wireless transmission using MIMO-OFDM visible-light communications," *IEEE Photonics Technology Letters*, vol. 25, no. 2, pp. 171–174, Jan. 2013.

[14] T. Q. Wang, Y. A. Sekercioglu, and J. Armstrong, "Analysis of an optical wireless receiver using a hemispherical lens with application in MIMO visible light communications," *IEEE/OSA Journal of Lightwave Technology*, vol. 31, no. 11, pp. 1744–1754, June 2013.

[15] Y.-J. Zhu, W.-F. Liang, J.-K. Zhang, and Y.-Y. Zhang, "Space-collaborative constellation designs for MIMO indoor visible light communications," *IEEE Photonics Technology Letters*, vol. 27, no. 15, pp. 1667–1670, Aug. 2015.

[16] J. Armstrong, "OFDM for optical communications," *IEEE/OSA Journal of Lightwave Technology*, vol. 27, no. 3, pp. 189–204, Feb. 2009.

[17] J. Vučić, C. Kottke, S. Nerreter, K.-D. Langer, and J. W. Walewski, "513 Mbit/s visible light communications link based on DMT-modulation of a white LED," *IEEE/OSA Journal of Lightwave Technology*, vol. 28, no. 24, pp. 3512–3518, Dec. 2010.

[18] A. M. Khalid, G. Cossu, R. Corsini, P. Choudhury, and E. Ciaramella, "1-Gb/s transmission over a phosphorescent white LED by using rate-adaptive discrete multitone modulation," *IEEE Photonics Journal*, vol. 4, no. 5, pp. 1465–1473, Oct. 2012.

[19] M. A. Khalighi, K. Raoof, and G. Jourdain, "Capacity of wireless communication systems employing antenna arrays, a tutorial study," *Wireless Personal Communications*, vol. 23, no. 3, pp. 321–352, Dec. 2002.

[20] A. J. Paulraj, D. A. Gore, R. U. Nabar, and H. Bolcskei, "An overview of MIMO communications: a key to gigabit wireless," *Proceedings of the IEEE*, vol. 92, no. 2, p. 198218, Feb. 2004.

[21] S. Long, M. A. Khalighi, M. Wolf, S. Bourenanne, and Z. Ghassemlooy, "Investigating channel frequency selectivity in indoor visible light communication systems," *IET Optoelectronics*, vol. 10, no. 3, pp. 80–88, May 2016.

[22] Z. Ghassemlooy, M. A. Khalighi, and D. Wu, *Visible Light Communications: Theory and Applications*. CRC-Press, 2017, ch. Channel Modeling, pp. 71–96.

[23] S. Weinstein, "The history of orthogonal frequency-division multiplexing," *IEEE Communications Magazine*, vol. 47, no. 11, pp. 26–35, Nov. 2009.

[24] J. Armstrong and B. J. C. Schmidt, "Comparison of asymmetrically clipped optical OFDM and DC-biased optical OFDM in AWGN," *IEEE Communications Letters*, vol. 12, no. 5, pp. 343–345, May 2008.

[25] S. Dimitrov, S. Sinanovic, and H. Haas, "Clipping noise in OFDM-based optical wireless communication systems," *IEEE Transactions on Communications*, vol. 60, no. 4, pp. 1072–1081, Apr. 2012.

[26] J. B. Carruthers and J. M. Kahn, "Multiple-subcarrier modulation for nondirected wireless infrared communication," *IEEE Journal on Selected Areas in Communications*, vol. 14, no. 3, pp. 538–546, Apr. 1996.

[27] S. Long, M. A. Khalighi, M. Wolf, Z. Ghassemlooy, and S. Bourenanne, "Performance of carrier-less amplitude and phase modulation with frequency domain equalization for indoor visible light communications," *International Workshop on Optical Wireless communications (IWOW)*, pp. 16–20, Sept. 2015, Istanbul, Turkey.

[28] D. Tsonev, S. Videv, and H. Haas, "Unlocking spectral efficiency in intensity modulation and direct detection systems," *IEEE Journal on Selected Areas in Communications*, vol. 33, no. 9, p. 17581770, Sept. 2015.

[29] F. B. Offiong, S. Sinanovic, and W. O. Popoola, "On PAPR reduction in pilot-assisted optical OFDM communication systems," *IEEE Access*, vol. 5, pp. 8916–8929, May 2017.

[30] W. Henkel, T. Kessler, and H. Chung, "Coded 64-CAP ADSL in an impulse-noise environment-modeling of impulse noise and first simulation results," *IEEE Journal on Selected Areas in Communications*, vol. 13, no. 9, pp. 1611–1621, Dec. 1995.

[31] R. Rodes, M. Wieckowski, T. T. Pham, J. B. Jensen, J. Turkiewicz, J. Siuzdak, and I. T. Monroy, "Carrierless amplitude phase modulation of VCSEL with 4 bit/s/Hz spectral efficiency for use in WDM-PON," *Optics Express*, vol. 19, no. 27, pp. 26 551–26 556, Dec. 2011.

[32] L. Tao, Y. Ji, J. Liu, A. P. T. Lau, N. Chi, and C. Lu, "Advanced modulation formats for short reach optical communication systems," *IEEE Network*, vol. 27, no. 6, pp. 6–13, nov 2013.

[33] G. Stepanik and J. Siuzdak, "Experimental investigation of PAM, CAP and DMT modulations efficiency over a double-step-index polymer optical fiber," *Optical Fiber Technology*, vol. 20, no. 4, pp. 369–373, Aug. 2014.

[34] R. Kruglov., S. Loquai, C.-A. Bunge, M.Schueppert, J. Vinogradov, and O. Ziemann, "Comparison of PAM and CAP modulation schemes for data transmission over Si-POF," *IEEE Photonics Technology Letters*, vol. 25, no. 23, pp. 2293–2296, Dec. 2013.

[35] F.-M. Wu, C.-T. Lin, C.-C. Wei, C.-W. Chen, H.-T. Huang, and C.-H. Ho, "1.1-Gb/s white-LED-based visible light communication employing carrier-less amplitude and phase modulation," *IEEE Photonics Technology Letters*, vol. 24, no. 19, pp. 1730–1732, Oct. 2012.

[36] F.-M. Wu, C.-T. Lin, C.-C. Wei, C.-W. Chen, Z.-Y. Chen, and H.-T. Huang, "Performance comparison of ofdm signal and CAP signal over high capacity RGB-LED-based WDM visible light communication," *IEEE Photonics Journal*, vol. 4, no. 4, Aug. 2013.

[37] G. Stepanik, L. Maksymiuk, and J. Siuzdak, "Experimental comparison of PAM, CAP, and DMT modulations in phosphorescent white LED transmission link," *IEEE Photonics Journal*, vol. 7, no. 3, pp. 1–8, June 2015.

[38] P. A. Haigh *et al.*, "Multi-band carrier-less amplitude and phase modulation for bandlimited visible light communications systems," *IEEE Wireless Communications*, vol. 22, no. 2, pp. 46–53, Apr. 2015.

[39] G.-H. Im, D. B. Harman, G. Huang, A. V. Mandzik, M.-H. Nguyen, and J.-J. Werner, "51.84 Mb/s 16-CAP ATM LAN standard," *IEEE Journal on Selected Areas in Communications*, vol. 13, no. 4, pp. 620–632, May 1995.

[40] D. Falconer, S. L. Ariyavisitakul, A. Benyamin-Seeyar, and B. Eidson, "Frequency domain equalization for single-carrier broadband wireless systems," *IEEE Communications Magazine*, vol. 40, no. 4, p. 5866, Apr. 2002.

[41] M. Wolf, L. Grobe, M. R. Rieche, A. Koher, and J. Vučić, "Block transmission with linear frequency domain equalization for dispersive optical channels with direct detection," in *12th IEEE International Conference on Transparent Optical Networks (ICTON)*, June 2010, pp. 1–8, Munich, Germany.

[42] M. Wolf, S. A. Cheema, M. A. Khalighi, and S. Long, "Transmission schemes for visible light communications in multipath environments," *ICTON Conference*, pp. 1–7, July 2015, Budapest, Hungary.

[43] D. Tsonev, S. Sinanovic, and H. Haas, "Complete modeling of nonlinear distortion in OFDM-based optical wireless communication," *IEEE/OSA Journal of Lightwave Technology*, vol. 31, no. 18, pp. 3064–3076, Sept. 2013.

[44] P. A. Haigh, A. Burton, K. Werfli, H. Le Minh;, E. Bentley, P. Chvojka, W. O. Popoola, I. Papakonstantinou, and S. Zvanovec, "A multi-CAP visible-light communications system with 4.85-b/s/Hz spectral efficiency," *IEEE Journal on Selected Areas in Communications*, vol. 33, no. 9, pp. 1771–1779, Sept. 2015.

[45] D. Tsonev, S. Videv, and H. Haas, "Towards a 100 Gb/s visible light wireless access network," *Optics Express*, vol. 23, no. 2, pp. 1627–1637, Jan. 2015.

[46] T. Ngo, "Why Wi-Fi stinks - and how to fix it," *IEEE Spectrum Magazine*, vol. 53, no. 7, pp. 44–50, July 2016.